

RESEARCH

Open Access



Multi-omics analysis reveals that *Bacillus* spp. enhance mucosal antiviral immunity in teleost fish by mediating diglyceride production through lipid metabolism

Gaofeng Cheng^{1,2†}, Weiguang Kong^{2†}, Ruiqi Lin², Zhihao Jiang³, Xinyou Wang², Xueying Qin², Yong Shi², Peng Yang², Xiaoyun Chen², Lu Xia¹ and Zhen Xu^{2*}

Abstract

Background Symbiotic microbiota in vertebrates play critical roles in establishing and enhancing host resistance to pathogenic infections as well as maintaining host homeostasis. The interactions and mechanisms of commensal microbiota-mediated mucosal immune systems have been extensively studied in mammals and, to a lesser extent, in birds. However, despite several studies emphasizing the role of mucosal microbiota in controlling pathogen infections in teleost fish, limited knowledge exists regarding the core microbiota and the mechanisms by which they contribute to resistance against viral infections.

Results Our findings suggest that viral infections shape clinical manifestations of varying severity in infected fish. An increased abundance of *Bacillus* spp. in the mild phenotype indicates its crucial role in influencing fish immunity during viral infections. To confirm that *Bacillus* spp. act as a core contributor against viral infection in fish, we isolated a representative strain of *Bacillus* spp. from largemouth bass (*Micropterus salmoides*), which was identified as *Bacillus velezensis* (Bv), and subsequently conducted feeding trials. Our study demonstrated that dietary supplementation with Bv significantly reduced mortality from largemouth bass virus (LMBV) infection in bass by enhancing host immunity and metabolism as well as by regulating the microbial community. Furthermore, multi-omics analysis elucidated the mechanism by which *Bacillus* spp. confer resistance to viral infections by regulating the production of diglyceride (DG) during lipid metabolism.

Conclusions Our study provides the first evidence that *Bacillus* spp. are a core microbiota for combating viral infections in teleost fish, shedding light on the conserved functions of probiotics as a core microbiota in regulating microbial homeostasis and mucosal immunity across the vertebrate lineage.

Keywords *Bacillus velezensis*, Symbiotic microbiota, Multi-omics analysis, Viral infection, Largemouth bass

[†]Gaofeng Cheng and Weiguang Kong contributed equally to this work.

*Correspondence:

Zhen Xu
zhenxu@ihb.ac.cn

Full list of author information is available at the end of the article



Background

Mucosal surfaces in vertebrates host a diverse and abundant community of commensal microbiota that are essential for maintaining host homeostasis. The biodiversity of the symbiotic microbiome is closely associated with the evolution of vertebrates, giving rise to host-specific microbiome characteristics and dynamic, complex interactions during coevolution [1]. In mammals, extensive evidence highlights the importance of commensal microbiota in shaping host innate immune systems, influencing pathogenic infections by regulating immune function and intestinal mucosal homeostasis, with the core microbiota serving as a key contributor [2–5]. Core microbiota, defined as the microbial taxa that are shared or abundant within the host, have been shown to play a crucial role in maintaining host health in mammals [6–9]. Currently, research on core microbial communities in avian and reptilian species is limited to classifications based on microbial abundance and shared taxa [10, 11]. Teleost fish represent the oldest extant bony vertebrates and harbor complex and abundant microbial communities on their mucosal surfaces. The susceptibility of teleost fish to opportunistic pathogens highlights the necessity to study the roles of mucosal microbes in early vertebrates. Mucosal microbiota associated with teleost fish have been studied extensively, and the shared core microbiota in fish mucosa have been reported in previous studies [12, 13]. However, studies investigating the resistance of mucosal core microbiota to pathogen infections in teleost remain scarce.

The core microbiota serves as both a holistic health indicator and a potential contributor to health improvement. Probiotics have garnered widespread attention for their contribution to maintaining intestinal microbiome homeostasis, enhancing intestinal barrier function, and regulating immune responses [14, 15]. A previous study in humans investigated the role of mucosal microbiota in infections, highlighting the loss of the core beneficial microbiota *Prevotella* spp. during acute viral infections [16]. Recently, several core microbiotas have been identified in mammals, including *Akkermansia*, *Bacteroides*, and *Faecalibacterium*, all of which are probiotics that are crucial for maintaining gut homeostasis and overall health [9, 17, 18]. Additionally, the core microbe *Bifidobacterium* in the gut of calves improves the growth phenotype of hosts by regulating microbial functions and host metabolism [19]. Studies involving mammals suggest that probiotics, with the potential to serve as core microbiota, contribute to the normalization of disrupted gut microbiota caused by viral stimulation or environmental stressors [20, 21]. In teleost fish, previous studies have examined the role of probiotics in mucosal homeostasis; however, evidence regarding the involvement of

core microbiota in pathogen resistance remains limited. Recent studies show that probiotics regulate the stability of the gut microbiota network, enhance microbial interactions, and promote resistance to pathogen infections in zebrafish [22]. The contributions of probiotics to host physiology are largely driven by secondary metabolites. This is consistent with findings from studies involving mammals, where metabolites produced by probiotics, such as bacteriocin, surfactin, and P34 peptide, protect hosts from viral infections by inhibiting viral binding, entry, and replication [23–25]. In teleost fish, an extract derived from *Bacillus* spp. has been shown to resist SVCV infection by enhancing the innate immune response [26]. Previous studies have demonstrated that *Bacillus velezensis* (Bv) enhances zebrafish immunity against pathogen infections by strengthening gut microbiome interactions, which are dependent on vitamin B12 produced by *Cetobacterium* [21]. Additionally, probiotics play a crucial role in regulating immune and metabolic networks by influencing the interactions between the mucosa and microbiota, particularly through the enhancement of lipid metabolism [27]. Notably, diglyceride (DG) has been identified as a key signaling lipid and an important intermediate in lipid metabolism [28]. Recent research in mammals suggests that DG activates multiple downstream signaling cascades, including the Ras, NF- κ B, and AKT pathways, thereby mediating T-cell immunity [29]. Despite growing evidence showing that specific symbiotic microbiotas in the mucosa protect hosts against pathogen infections, a comprehensive understanding of the core microbiota and the specific mechanism underlying pathogen resistance in teleost fish is lacking.

To address this gap in the literature, this study investigated the core microbiota and the specific mechanisms of their contributions to antiviral defense in teleost fish. We utilized largemouth bass as an experimental model and defined differential phenotypes following largemouth bass virus (LMBV) infection. Subsequently, the composition of symbiotic microbiota in the gut of largemouth bass exhibiting mild and severe phenotypes was analyzed using 16 s rRNA sequencing. Our results indicated that *Bacillus* spp. may represent the core microbiota mediating early antiviral responses in the largemouth bass. To confirm this hypothesis, we isolated a representative strain of the *Bacillus* spp. from bass, which was identified as Bv, and subsequently observed that Bv supplementation provided protection against viral infection. Subsequently, we investigated the effects of Bv supplementation on the composition and structure of the intestinal microbiome, exploring the correlation between alterations in the microbiota and host metabolism and immunity through multi-omics association analysis.

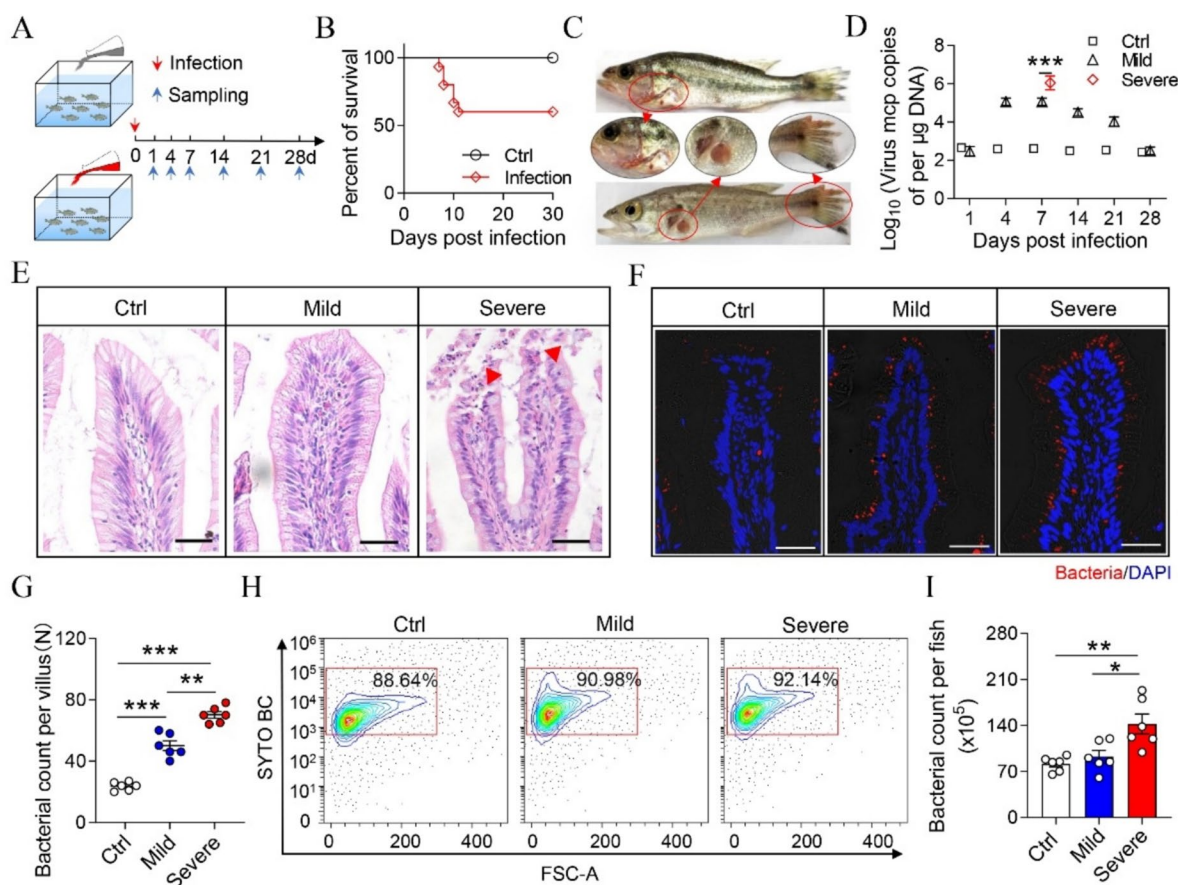


Fig. 1 Infection model and microbial abundance analysis. **A** Fish were infected with LMBV via bath immersion and sacrificed at 1, 4, 7, 14, 21, and 28 DPI for tissue sample collection. **B** Cumulative survival rate of the Ctrl group and LMBV-infected group. The data are representative of two independent experiments. **C** Clinical phenotypes observed in largemouth bass infected with LMBV. **D** qPCR was used to quantify LMBV mcp gene copies (Log_{10}) in the gut samples from the Ctrl, Mild, and Severe groups ($n = 6$). **E** Histological examination of the gut in Ctrl, Mild-7, and Severe-7 group fish. **F** Distribution of bacteria in gut paraffin sections from fish in the Ctrl, Mild, and Severe groups was detected by in situ hybridization. From left to right: Ctrl, Mild, and Severe groups, scale bars: 30 μm . **G** Bacterial counts per villus in the Ctrl, Mild, and Severe groups ($n = 6$). Statistical differences were evaluated using a one-way ANOVA test. **H** Flow cytometry analysis displaying the staining of gut bacteria with SYTO BC Green in the Ctrl, Mild, and Severe groups. **I** The total gut bacterial count per fish in the Ctrl, Mild, and Severe groups ($n = 6$). * $p < 0.05$, ** $p < 0.01$, *** $p < 0.001$

Furthermore, we identified a mechanism by which Bv enhances host resistance to viral infections via lipid metabolism, specifically through DG. These results demonstrate that *Bacillus* spp. may serve as a core microbiota that mediates early antiviral responses in teleosts, supporting host immunity by regulating the production of DG during lipid metabolism. Overall, our results indicate that the conserved role of probiotics as core microbiota in antiviral immunity in both primitive and modern vertebrates is through a process of convergent evolution.

Results

LMBV infection induced differential clinical symptoms and gut microbiota disruption

In this study, we evaluated the immune responses of largemouth bass by developing a bath infection model with LMBV. Infected fish were sacrificed to collect samples at 1-, 4-, 7-, 14-, 21-, and 28-day post-infection (DPI) (Fig. 1A). Approximately, 40% of the fish succumbed to LMBV infection (Fig. 1B). Infected fish displayed typical clinical phenotypes, including spleen enlargement, skin ulcers, and fin congestion (Fig. 1C). At 7 DPI, infected fish exhibited variable clinical phenotypes. Based on the pathological phenotypes, infected fish were categorized into Mild and Severe groups (Supplementary Fig. 1A). qPCR analysis revealed that LMBV loads in the gut

increased significantly at 4 DPI and remained elevated at 7 DPI, similar to the LMBV load patterns in the head kidney (HK) (Fig. 1D, Supplementary Fig. 1B). Notably, fish in the Severe group exhibited a higher LMBV load compared to those in the Mild group. H&E staining identified morphological changes in the Severe group, including cell shedding around the gut villi, while no significant changes were observed in the Mild group (Fig. 1E). The expression levels of antiviral genes (*irf-7*, *irf-3*, *ifn α* , *trim25*, and *mx*) and inflammation-related genes (*il-10*, *il-8*, and *il-1 β*) were increased at 1 and 4 DPI before gradually decreasing at 7 DPI. Fish in the Severe group exhibited a stronger upregulation of immune-related genes compared to those in the Mild group (Supplementary Fig. 1D). Moreover, bacteria of the gut mucosa were visualized using fluorescent in situ hybridization analysis. The results revealed a significant increase in microbial abundance in the Mild and Severe groups compared to the control (Ctrl) group (Fig. 1F, G). Flow cytometry further confirmed this increase in microbial abundance in the gut, with fish in the Severe group exhibiting a greater microbial abundance in the gut than fish in both the Ctrl and Mild groups (Fig. 1H, I; samples that were not stained with SYTO BC Green are shown in Supplementary Fig. 1D). These findings suggest that LMBV invasion elicits strong immune responses and disrupts the gut microbiota of largemouth bass.

Bacillus spp. mediate the early antiviral immune response of largemouth bass

To investigate microbial composition in the Mild and Severe groups, gut samples were collected from fish in the Ctrl, Mild, and Severe groups for 16S rRNA sequencing analysis. The Chao1 index showed that the bacterial community richness in the severe group was significantly higher than in the mild group, and it was also elevated compared to the control group (Fig. 2A). Principal component analysis (PCA) indicated that the microbiome pattern in the Ctrl group was similar to that in the Mild group but differed from that of fish in the Severe group (Fig. 2B). At the genus level, the composition of the microbiota varied significantly among fish in the Ctrl, Mild, and Severe groups (Fig. 2C). BugBase analysis indicated a higher abundance of pathogenic and facultatively anaerobic bacteria in the Severe group compared to those in the Ctrl group, whereas fish in the Mild group exhibited no significant changes (Fig. 2D, E). Heat map analysis highlighted distinctions in the composition of pathogens and probiotics among the three groups. Fish in the Severe group showed a marked increase in the relative abundance of pathogenic bacteria and a decrease in probiotics. Fish in the Mild group exhibited a modest increase in the relative abundance of probiotics compared to the

Ctrl fish (Fig. 2F). Specifically, a significant increase in pathogenic bacteria such as *Aeromonas* and *Plesiomonas* was observed in Severe group fish, accompanied by a notable decline in probiotics, particularly *Lactobacillus* (Fig. 2G). In contrast, fish in the Mild group displayed a significant increase in *Bacillus* spp. compared to both the Ctrl and Severe groups, suggesting that *Bacillus* spp. may play an important role in resistance to LMBV infection in largemouth bass. To further evaluate the potential mechanisms by which *Bacillus* spp. mediate the immune response of bass against LMBV invasion, we isolated *Bacillus* spp. from the gut of largemouth bass and identified it as *B. velezensis* (Bv). Subsequently, our findings demonstrated that this strain inhibited the growth of pathogenic bacteria, including *Aeromonas hydrophila*, *Edwardsiella piscicida*, and *Nocardia seriolae* (Supplementary 2A, B). Additionally, the strains exhibited the potential to enhance nutrient utilization through the production of enzymes such as protease, cellulase, amylase (AMS), and lipase (LPS) (Supplementary Fig. 2C).

Bv supplementation enhanced growth performance and antiviral ability of bass

To evaluate the role of strain Bv in bass, the fish were fed a commercial diet supplemented with Bv for 28 days (Fig. 3A). Results showed that the feed coefficient in the Bv group significantly decreased, whereas the weight gain rate (%) and specific growth rate (%/d) significantly increased compared to the Ctrl group (Fig. 3B). Moreover, significant improvements in the characteristics of the foregut (FG) and midgut (MG) villi were observed, including the increased villus length, villus count, and muscle layer thickness compared to the Ctrl group (Supplementary Fig. 3A, B). A significant increase in the trypsin (TPS), AMS, and LPS activities was observed in the FG of the Bv group. Additionally, TPS activity increased in the MG and LPS activity increased in the hindgut (HG) of the Bv group (Fig. 3C). Furthermore, increased activities of innate immune-related enzymes, including superoxide dismutase (SOD), lysozyme (LSZ), and acid phosphatase (ACP), were observed in the gut and serum (Fig. 3D, Supplementary Fig. 3C). Collectively, our findings demonstrated that Bv supplementation effectively enhanced the activities of both digestive and innate immune-related enzymes. To further investigate whether supplementation with Bv provides protection against LMBV infection in largemouth bass, we developed an intraperitoneal infection model. Our results indicated that approximately 60% of fish in the Ctrl group and 40% of fish in the Bv-fed group died within 30 days (Fig. 3E). qPCR analysis revealed that the LMBV load in the spleen (SP), FG, and HG of the Bv group was significantly lower at 7 DPI compared to the

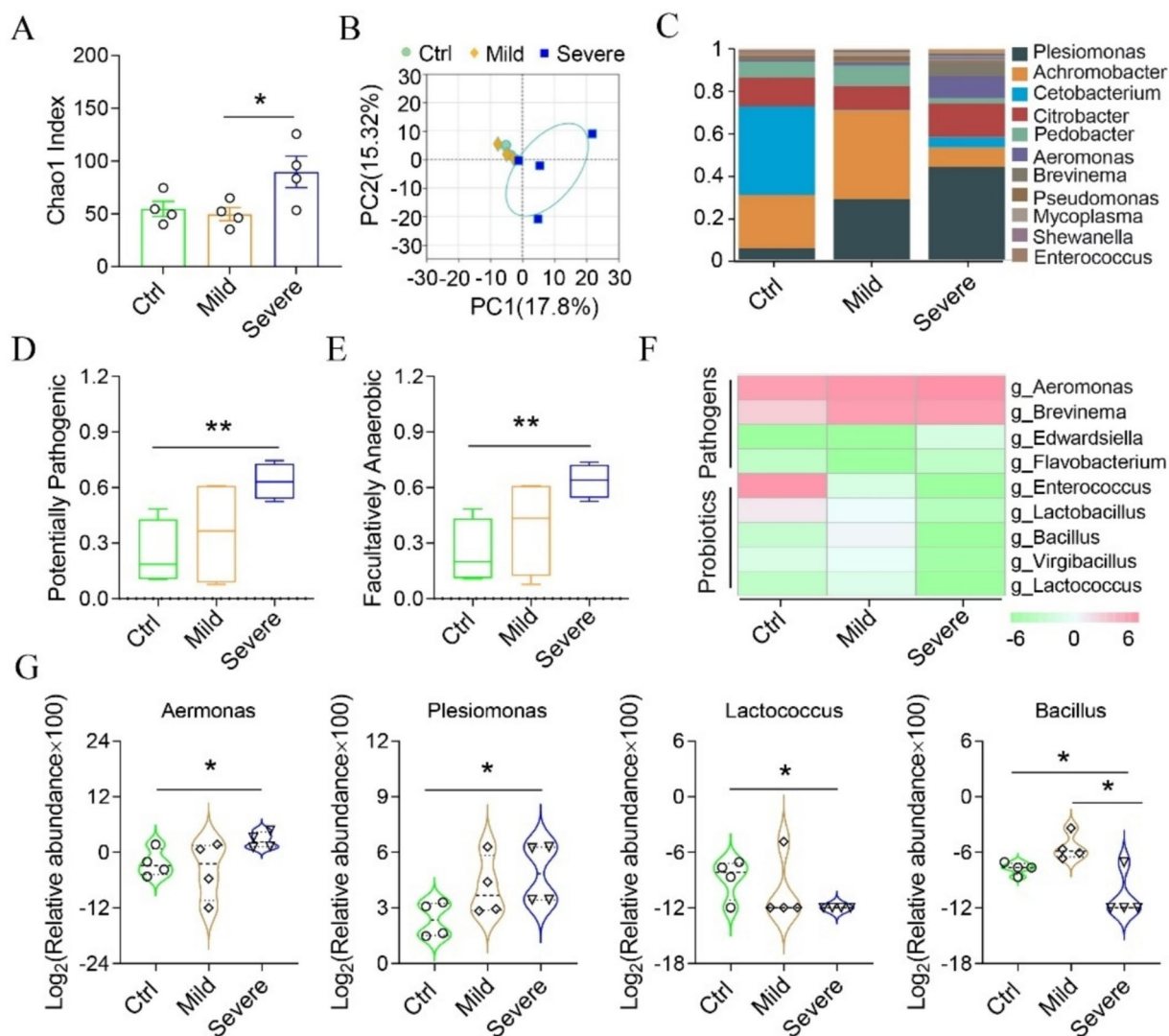


Fig. 2 Composition differences in gut commensal microbiota among fish in the Ctrl, Mild, and Severe groups ($n = 4$ samples, three fish per sample). **A** Microbial richness in the gut of fish in the Ctrl, Mild, and Severe groups ($n = 4$). Community richness was measured using the Chao1 index. **B** PCA analysis was performed to assess the gut microbiome communities of fish in the Ctrl, Mild, and Severe groups ($n = 4$). **C** Relative abundance of gut microbiota at the genus level in fish in the Ctrl, Mild, and Severe groups. **D, E** Proportions of potentially pathogenic (D) and facultatively anaerobic bacteria (E) in the Ctrl, Mild, and Severe groups fish. **F** Heatmap displays the relative abundance of pathogenic bacteria and probiotics in Ctrl, Mild, and Severe fish (Log_2 relative abundance). **G** Relative abundance of specific microbiota (*Aeromonas*, *Shewanella*, *Lactococcus*, and *Bacillus*) in the Ctrl, Mild, and Severe groups fish

Ctrl group (Fig. 3F). Additionally, we defined the pathological phenotypes of infected fish at 7DPI and recorded the percentages of asymptomatic (Non), Mild, and Severe phenotypes in the Ctrl and the Bv group (Supplementary Fig. 3D). In the Bv group, the proportions were 66.7%, 19.4%, and 13.9%, compared to 52.8%, 27.8%, and 19.4% in the Ctrl group (Fig. 3G). This suggests that Bv supplementation alleviates clinical symptoms after LMBV infection and enhances the antiviral resistance of large-mouth bass.

Bv supplementation induced differential immune responses in the intestinal segment

To analyze the immune responses of the gut following Bv supplementation, we performed transcriptome sequencing analysis on the FG, MG, and HG after 28 days of Bv supplementation. We found a total of 602 genes (FG), 604 genes (MG), and 1080 genes (HG) were differentially expressed following Bv supplementation. Among these genes, 234, 346, and 378 genes were downregulated, whereas 368, 258, and 702 genes were upregulated

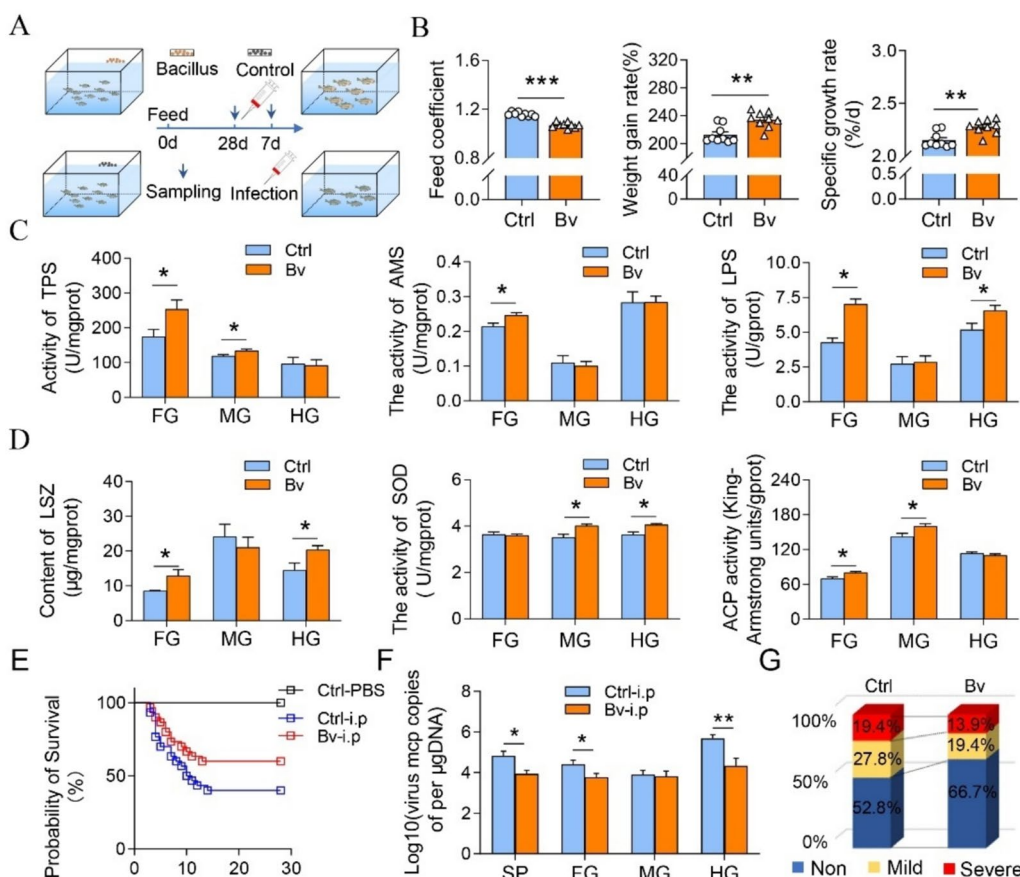


Fig. 3 Supplementation with Bv enhanced host nutrition utilization and immunity against LMBV infection. **A** Experimental strategy: fish were fed a diet supplemented with Bv for 28 days, and 20 fish were randomly selected and sacrificed for tissue sample collection. The remaining fish were injected with LMBV, with 30 fish used for the mortality test and 60 fish that were subjected to phenotypic analysis and tissue sample collection at 7 DPI. **B** Effects of dietary Bv on growth performance of largemouth bass (feed coefficient, weight gain rate, and specific growth rate). **C** Effect of dietary supplementation with Bv on TPS, AMS, and LPS in the FG, MG, and HG of largemouth bass. **D** Effect of dietary supplementation with Bv on LSZ, SOD, and ACP activity in the FG, MG, and HG of largemouth bass. **E** Cumulative survival rates of fish in the Bv and Ctrl groups following LMBV intraperitoneal injection (abbreviations: Ctrl-i.p and Bv-i.p). The data are representative of two independent experiments. **F** LMBV mcp copies (Log_{10}) in SP, FG, MG, and HG of fish ($n = 6$). **G** Statistical analysis of differential phenotypes of infected fish in the Ctrl group and Bv-fed group. The red section indicates the proportion of severely diseased fish, the yellow section represents the proportion of mildly diseased fish, and the blue section represents the proportion of asymptomatic (non-phenotypic: non) fish. * $p < 0.05$, ** $p < 0.01$, *** $p < 0.001$

in FG, MG, and HG, respectively (Fig. 4A). Additionally, 9 genes were upregulated in all 3 tissues, and 27 genes were downregulated (Fig. 4B). Furthermore, we observed that immune-related genes were significantly upregulated in FG, MG, and HG following Bv supplementation (Fig. 4C). Genes associated with metabolic function were also upregulated in FG, MG, and HG compared to the Ctrl group (Fig. 4D). KEGG enrichment analysis revealed that differentially expressed genes (DEGs) were enriched in pathways related to metabolism, immunity, and cellular proliferation (Fig. 4E). Notably, immune-related pathways, including the B-cell receptor signaling pathway and the NF- κ B signaling pathway, are enriched with more genes in the MG and HG (Fig. 4E). These findings

highlight the important role of the MG and HG as potential targets for induced intestinal immunity following Bv supplementation in largemouth bass.

Bv supplementation affected the composition and structure of symbiotic microbiota in the intestinal segment

To investigate the effects of Bv feeding on the structure and composition of the gut microbiota in largemouth bass, the FG, MG, and HG were collected for 16S sequence analysis. The Chao1 index indicated a significant increase in bacterial community richness in the HG of the Bv group compared to the Ctrl group (Fig. 5A). Consistently, the OTU analysis indicated that the number

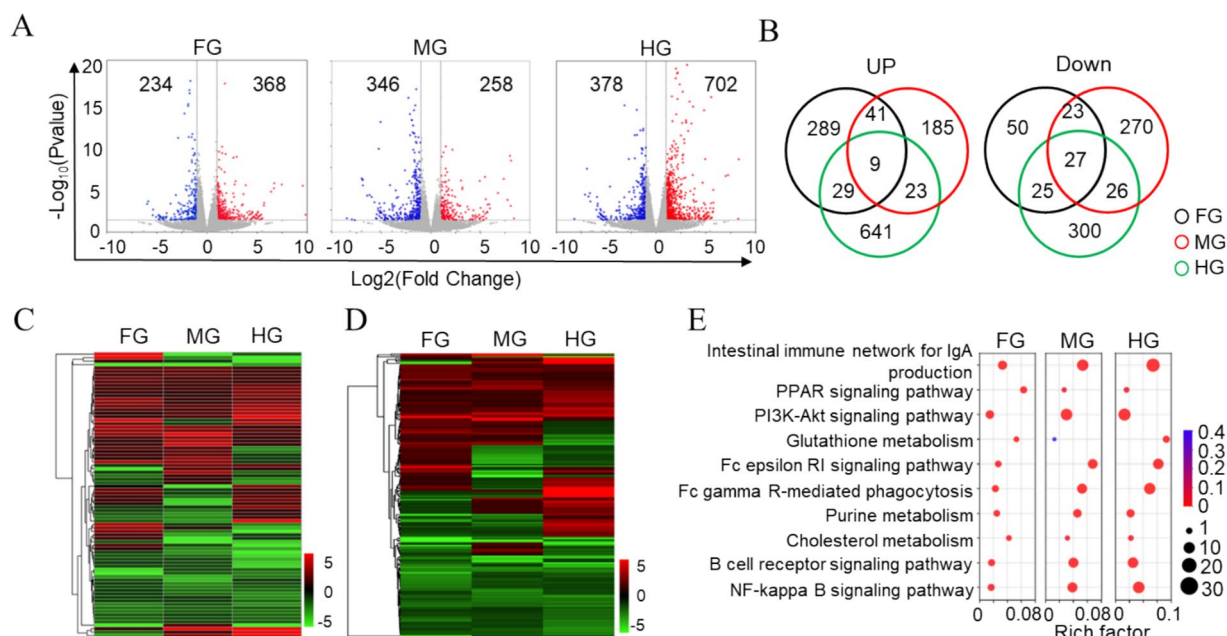


Fig. 4 Transcriptomic analysis of bass gut tissues following Bv supplementation ($n = 3$ samples, three fish per sample). **A** Volcano plot shows the upregulated or downregulated expression of genes in FG, MG, and HG of Bv-group fish versus Ctrl fish. Red dots indicate significantly upregulated genes (fold change > 2 and $FDR < 0.05$), blue dots indicate significantly downregulated genes (fold change < 2 and $FDR < 0.05$), and grey spots indicate no differential expression. **B** Venn diagrams show the overlap of upregulated or downregulated genes across FG, MG, and HG. **C** Heatmap of RNA-Seq analysis shows changes in immune-related genes from the FG, MG, and HG of Bv-group fish versus Ctrl fish. **D** Heatmap of RNA-Seq analysis shows changes in metabolic-related genes from the FG, MG, and HG of Bv-group fish versus Ctrl fish. **E** KEGG analysis revealed significant changes in biological processes in the FG, MG, and HG of Bv-group fish versus Ctrl fish

of OTUs in the HG of the Bv (78) group increased compared to the Ctrl group (34), with nine specific OTUs (Supplementary Fig. 4). Additionally, the OTU number in the FG and MG was higher than in the HG, with the total OTU number in the FG group being the highest (Supplementary Fig. 4). Moreover, the variation in bacterial structure at the phylum and family levels can be visually depicted from the circo plot analysis (Fig. 5B, C). At the phylum level, the relative abundance of Proteobacteria decreased in FG and MG, and there was an increase in the relative abundance of Firmicutes and Bacteroidota in the HG (Fig. 5D). Meanwhile, we observed a significant decrease in the abundance of Enterobacteriaceae and an increase in Fusobacteriaceae in the FG. In the MG, Aeromonadaceae significantly decreased. Additionally, the abundance of Mycoplasmataceae and Alcaligenaceae increased significantly in the HG (Fig. 5E). LEfSe analysis further evaluated the changes in the microbial community composition at the genus level. We found that Bv feeding led to more pronounced changes in the microbial composition and structure of the HG compared to the FG and MG. Furthermore, the abundance of pathogenic bacteria, such as *Aeromonas*, decreased in the MG and HG following Bv supplementation. Meanwhile, there was a significant increase in probiotic abundance, including

Cetobacterium in the FG and *Bacillus* in the HG, respectively. These results suggest that Bv supplementation regulates the structure and composition of the gut microbiota, thereby providing benefits to gut health (Fig. 5F, G, H).

Bv supplementation regulates metabolic function of intestinal segment

PCA analysis indicated that distinct separations of metabolites in the FG, MG, and HG exist between the Ctrl and Bv groups (Fig. 6A). The Venn diagram illustrates the number of different metabolites in the FG, MG, and HG, revealing total metabolite counts of 133, 162, and 313, respectively (Fig. 6B). $VIP > 1$ indicates that the metabolite has a high impact on this group. In our study, several metabolites in the FG were significantly upregulated compared to the Ctrl group ($VIP > 1$), including D-ribose 5-phosphate, leukotriene E4, isopenicillin N, vitamin B6, 5-hydroxy-L-tryptophan, L-tryptophan, and ornithine. Notably, adenosine monophosphate, thiamine pyrophosphate, and 3',5'-cyclic GMP showed marked downregulation in Bv-fed fish (Fig. 6C). The enriched pathways of differential metabolites in the FG mainly related to metabolism, including vitamin B6 metabolism, purine metabolism, tryptophan metabolism, and

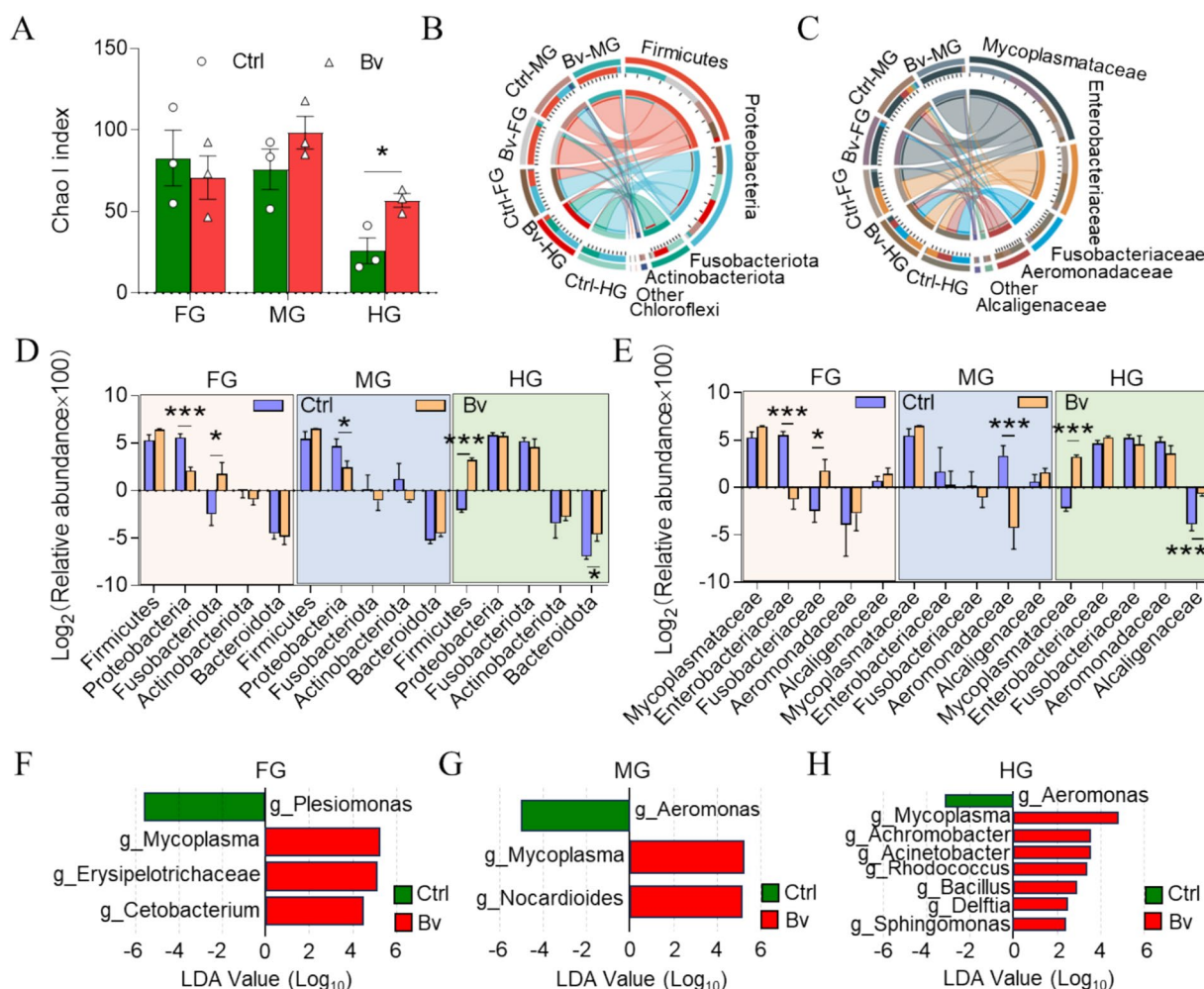


Fig. 5 Bv supplementation altered the microbial diversity and composition in the FG, MG, and HG ($n = 3$ samples, three fish per sample). **A** Richness of microbiota in FG, MG, and HG ($n = 3$). Community richness was measured by the [LE1] Chao1 index. **B, C** Circos plots showing the microbial abundance in FG, MG, and HG at the phylum (**B**) and family (**C**) levels. **D, E** Relative abundance (%) of the top five bacteria (phylum and family) in the FG, MG, and HG. **F, G, H** LEfSe cladogram of microbial taxa in FG (**F**), MG (**G**), and HG (**H**) of fish in the Ctrl and Bv groups (genus). * $p < 0.05$, ** $p < 0.01$, *** $p < 0.001$

aldosterone synthesis and secretion (Fig. 6F). Bv supplementation resulted in the upregulation of metabolites such as lysophosphatidylcholine (LysoPC), leukotriene F4, 5-trans-PGE2, glycerophosphoric acid, 9-hydroxylinoleic acid, and PE-NMe2 in MG. Conversely, prostaglandin E2, D-galactose, and 12-oxo-ETE were significantly downregulated in the Bv group compared to the Ctrl group. Furthermore, these differential metabolites were significantly enriched in pathways including glycerophospholipid metabolism and arachidonic acid metabolism (Fig. 6D, G). Additionally, metabolites such as 9-hydroxylinoleic acid, diglyceride (DG), and phosphatidylcholine (PC) were upregulated in the HG of the Bv group compared to the Ctrl group. Notably, these differential metabolites were enriched in pathways including linoleic

acid metabolism, glycerophospholipid metabolism, NF- κ B signaling pathway, and PPAR signaling pathway (Fig. 6E, H).

Correlation analysis of multiple omics sequencing revealed that Bv supplementation enhanced immune-related pathways

A correlation analysis of metabolomics and 16S sequencing was performed to investigate the relationship between the differential microbiota and secondary metabolites (Fig. 7A, B, C). Spearman's correlation analysis indicated that *Cetobacterium* was positively correlated with vitamin B6 in the FG (Fig. 7A). A negative correlation was observed between *Aeromonas* and Geneticin in the HG, and *Bacillus* exhibited a positive correlation with DG

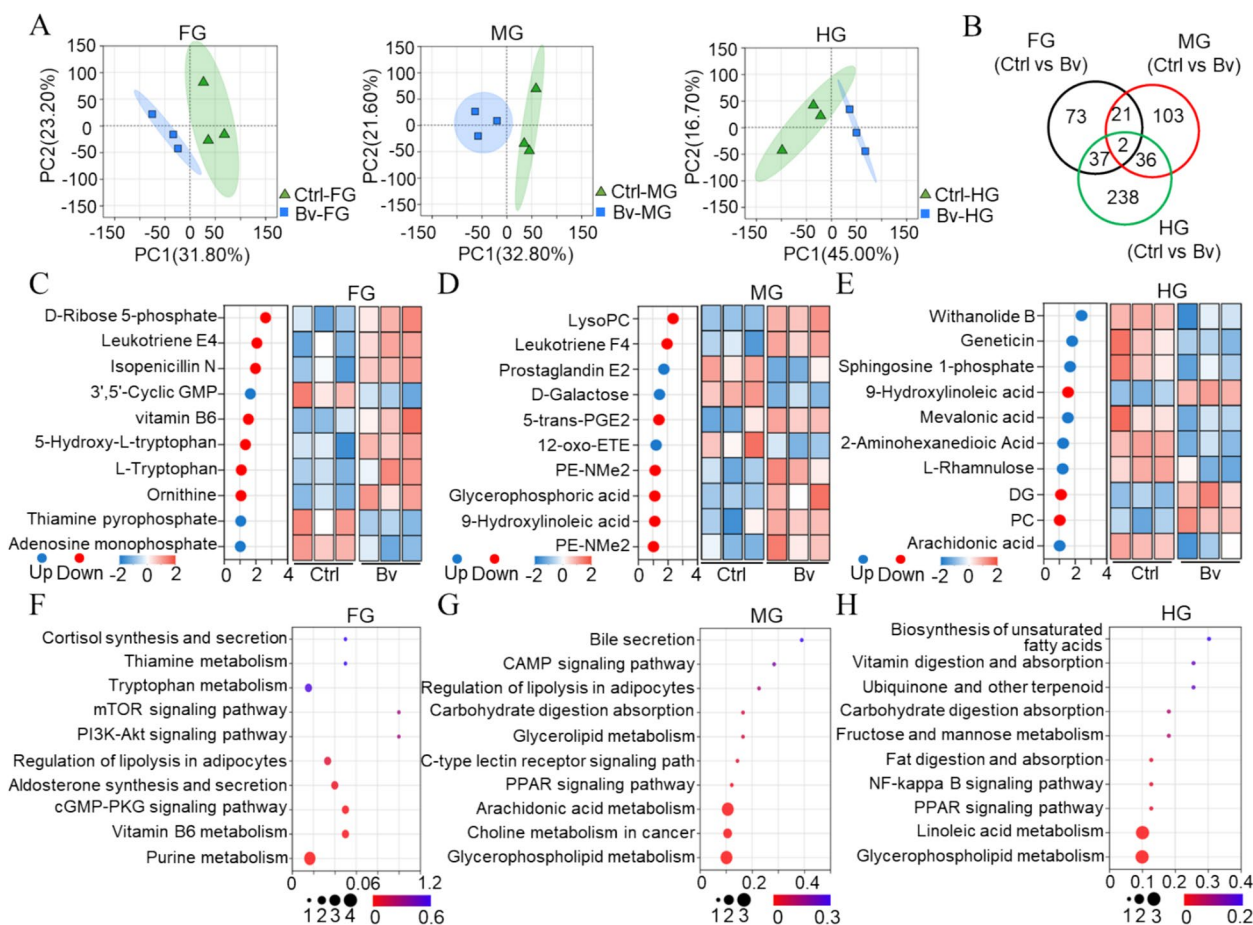


Fig. 6 Differential metabolite analysis of the FG, MG, and HG in the Ctrl and Bv groups ($n = 3$ samples, three fish per sample). **A** PCA analysis was performed to assess the metabolite composition of fish in the Ctrl, Mild, and Severe groups. **B** Venn diagram shows the overlap of metabolites in the FG, MG, and HG of the Ctrl and Bv groups. **C, D, E** Comparison of differential metabolites in the FG (**C**), MG (**D**), and HG (**E**) between the Ctrl and Bv groups. The dot plots on the left show VIP scores from the multivariate analysis, and the heatmaps on the right represent the relative levels of each metabolite across the Ctrl and Bv groups. **F, G, H** Bubble plots show the pathways of metabolite enrichment in the FG (**F**), MG (**G**), and HG (**H**). Bubble size indicates the number of metabolites in each pathway, while color represents the p -value

and 9-hydroxylinoleic acid in the HG (Fig. 7C). Genome sequencing further confirmed that Bv can produce lipases to regulate lipid metabolism and mediate DG production (Supplementary Fig. 5). Furthermore, other pathogens, including *Achromobacter* and *Mycoplasma*, exhibited a negative correlation with DG (Fig. 7C). Subsequently, the correlation analysis of metabolomics and transcriptome sequencing demonstrated that altered genes and metabolites are co-enriched into the same pathway (Fig. 7D, E, F). Furthermore, no significantly enriched pathways were observed in the FG, whereas the pathway of arachidonic acid metabolism was significantly enriched in the MG (Fig. 7D, E). Additionally, a significant correlation was observed in the HG between immune and metabolism-related pathways including phospholipase D signaling pathway, Fc epsilon RI signaling pathway, Fc gamma R-mediated phagocytosis, protein digestion

and absorption, and NF- κ B signaling pathway (Fig. 7F). Importantly, DG is a shared metabolite in the enriched immune and signaling transduction-related pathways of the HG (Table S2), which indicates that DG may mediate the immune response in the gut.

DG enhanced the protective effect of largemouth bass against LMBV infection

To determine whether the protective effects of Bv on the prevention of viral infection are reliant on DG, the EPC cells were incubated with M199 medium and M199 medium containing DG at a concentration of 0.5% for 2 h (Fig. 8A). qPCR analysis showed that DG incubation significantly enhanced the gene expression of *ifna*, *isg15*, and *mx*, whereas *viperin* did not exhibit significant variation, suggesting that DG might induce the antiviral function of EPC (Fig. 8B). After LMBV infection, the cytoplasmic

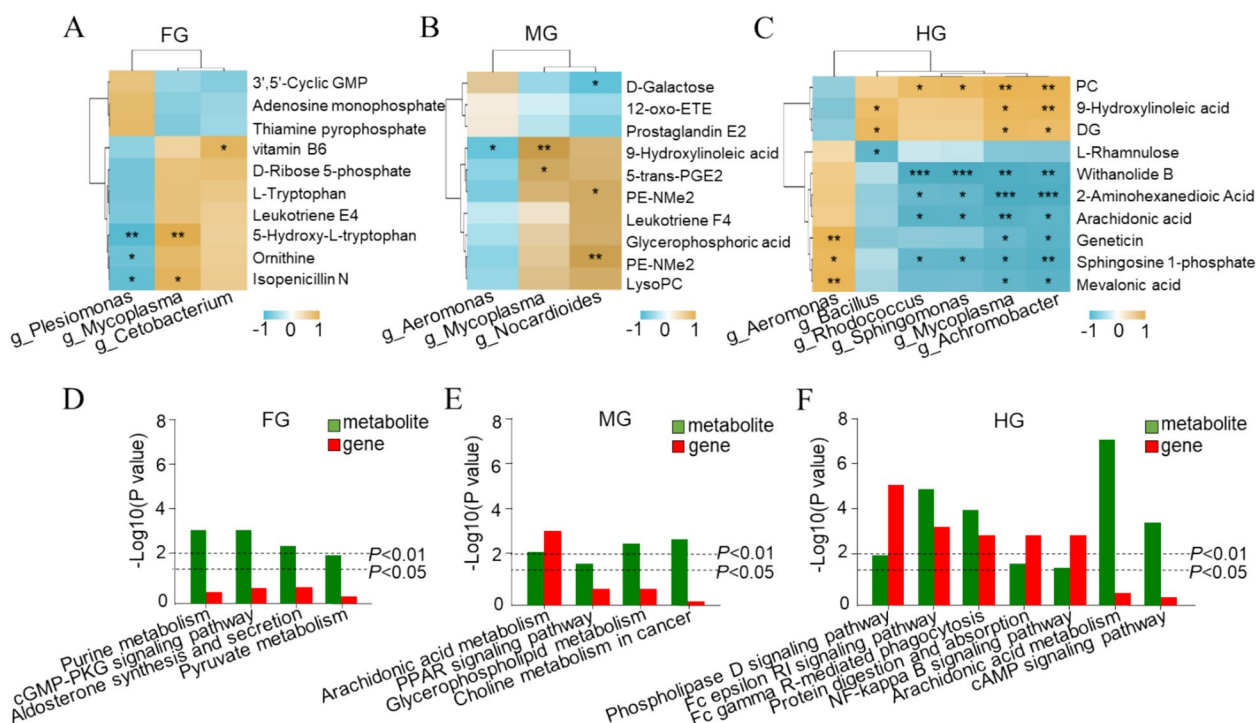


Fig. 7 Correlation analysis between differential metabolites, microbiota, and genes. **A, B, C** Heatmaps depicting correlations between microbial genera and metabolites in the FG (**A**), MG (**B**), and HG (**C**). The color indicates the degree of correlation, with yellow representing positive correlations and blue indicating negative correlations. **D, E, F** The bar chart shows significant correlations of enrichment pathways between metabolites in FG (**D**), MG (**E**), and HG (**F**) and genes ($*p < 0.05$, $**p < 0.01$, $***p < 0.001$)

effect (CPE) area was significantly reduced in the 0.5% DG group compared to the Ctrl group (Fig. 8C, Supplementary Fig. 6A). Subsequently, cells were collected after culture for 12 h for LMBV load analysis. We observed a lower LMBV load in EPCs incubated with DG compared to the Ctrl group (Fig. 8D). These results suggest that DG incubation induces the expression of antiviral genes in EPCs, thereby contributing to enhanced resistance to LMBV infection. To further explore the function of DG in defending against LMBV infection in largemouth bass, we designed an experiment involving feeding DG to analyze the protective effects of DG on largemouth bass (Supplementary Fig. 6B). Our results showed that the largemouth bass of the DG group with LMBV intraperitoneal injection (DG-i.p) presented higher survival rates compared to the PBS group with LMBV intraperitoneal injection (PBS-i.p) (Fig. 8E). The LMBV load in the SP, HK, FG, and HG significantly decreased in the DG-i.p group (Fig. 8F). H&E staining confirmed that DG supplementation alleviated the histopathology of the gut caused by LMBV infection, such as intestinal epithelial cell shedding and erythrocyte infiltration (Fig. 8G). Additionally, the statistics of pathological phenotypes showed that the proportions of Non-, Mild-, and Severe-phenotype fish were 66.7%, 11.1%, and 22.2% in the DG-i.p group,

compared with 35.0%, 25.0%, and 40.0% in the PBS-i.p group, respectively (Fig. 8H). In conclusion, the above results suggest that DG plays an important role in alleviating clinical symptoms and enhancing the resistance of largemouth bass against LMBV infection.

Discussion

Symbiotic bacteria coexist on mucosal surfaces and collaboratively maintain host health in vertebrates, with the core microbiota serving as a key contributor. However, the roles of core microbiota have mainly been investigated in mammals, whereas little is known regarding the core microbiota and its interactions with the mucosa during viral infection in teleost fish. In this study, we identified *Bacillus* spp. as a core contributor that mediates the clinical symptoms of early antiviral infection in largemouth bass. Furthermore, multi-omics analysis revealed the mechanisms through which Bv enhances antiviral infection resistance in largemouth bass, primarily through lipid metabolite DG that improves the host's immune response. Therefore, our results provide the first demonstration in teleost fish that probiotics, as core microbiota, exert conserved functions in regulating microbial homeostasis and mucosal immunity, thereby

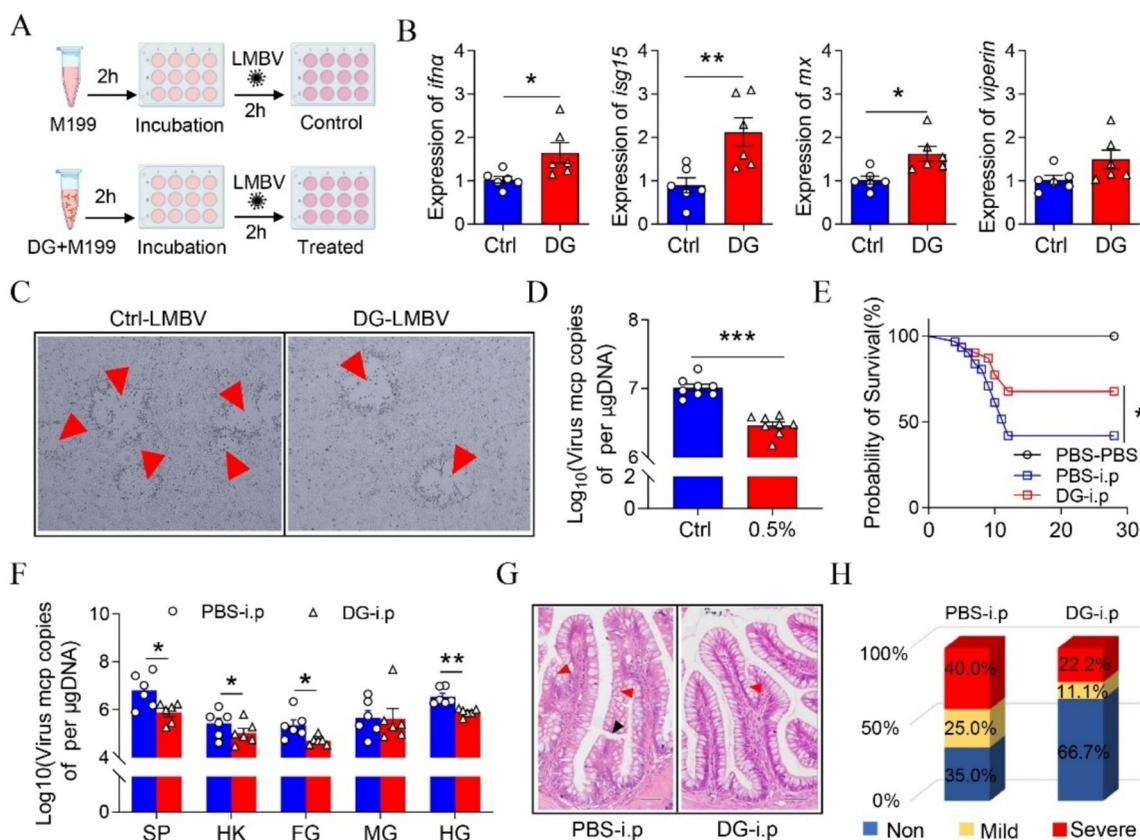


Fig. 8 DG enhances antiviral infection in vivo and in vitro. **A** Scheme of the DG antiviral experiment in vitro. **B** qPCR was used to detect the gene expression (*ifna*, *isg15*, *mx*, and *viperin*) in EPC cells from the 0.5% DG group and Ctrl group ($n = 6$). **C** The cytopathic effect (CPE) of EPC cells. **D** qPCR was used to detect LMBV mcp gene copies (Log_{10}) in EPC cells from the 0.5% DG and Ctrl group ($n = 8$). **E** Cumulative survival rates of fish in the DG (0.5%) and Ctrl group following LMBV intraperitoneal injection (abbreviations: DG-i.p and PBS-i.p). The data are representative of two independent experiments. **F** qPCR was used to detect LMBV mcp gene copies (Log_{10}) in the SP, HK, FG, MG, and HG from the DG-i.p and PBS-i.p groups ($n = 6$). **G** Histological examination of the gut in PBS-i.p and DG-i.p group fish using H&E staining, scale bars: 20 μm . **H** Statistical analysis of differential phenotypes of infected fish in the Ctrl group and DG-fed group. The red section represents the proportion of severely diseased fish, the yellow section represents the proportion of mildly diseased fish, and the blue section represents the proportion of non-phenotypic fish ($*p < 0.05$, $**p < 0.01$, $***p < 0.001$)

filling the gap in our understanding of mucosal microbiota function and evolution across the vertebrate lineage.

To assess the microbial composition of the intestinal mucosa after viral infection, we developed an LMBV infection model in bass via bath exposure, which mimics a natural infection. Defining phenotypes is essential for disease detection and evaluation. In our study, fish were classified into mild and severe infection categories based on the degree of clinical phenotypes, such as splenomegaly, extensive skin ulcers, local hemorrhaging, muscle necrosis, and swelling and ulcers at the fin base at 7 DPI [30]. Innate parameters are an important component of antiviral immune defense in aquatic animals [31, 32]. qPCR analysis revealed that fish with a severe phenotype exhibited elevated expression levels of antiviral genes (*irf-3*, *irf-7*, *trim25*, and *mx*) and inflammation-related genes (*il-8*, *il-1 β*) compared to fish with a mild phenotype,

accompanied by higher viral loads in the severe individuals. This finding is consistent with observations in humans where individuals with severe clinical phenotypes tend to have high viral loads and elevated levels of inflammatory genes [33–35]. Moreover, the inflammatory response caused by viral invasion can increase susceptibility to secondary bacterial infections and disrupt the microbial balance, resulting in a significant imbalance between beneficial and pathogenic bacteria [36–38]. Consistently, we found that the relative abundance of potential pathogenic and facultatively anaerobic bacteria was significantly increased in the Severe group compared to the Mild and Ctrl groups. Notably, most life-threatening pathogenic bacteria are facultative anaerobes [39]. Additionally, we observed that the abundance of beneficial *Bacillus* spp. was significantly higher in the Mild group fish. The microbiota differences in mild and severe

clinical phenotype groups suggest the important role of these bacterial communities in host health. It should be noted that host health is the outcome of the combined effects of multiple factors, including nutrition, lifestyle, and genetic background [40]. Studies have shown that host genetics influence the composition of microbiota and play a crucial role in both directly and indirectly regulating disease susceptibility [41]. However, this study is limited to investigating the impact of the microbiome on the host's susceptibility to viral infections. It is hypothesized that *Bacillus* species may serve as a potential core microbiota that alleviates pathological phenotypes and maintains health in largemouth bass following LMBV infection. Consistent with previous studies, several bacterial communities with beneficial effects, including *Prevotella* spp., *Akkermansia* spp., *Bacteroides* spp., and *Faecalibacterium* spp., have been reported as core microbiota in mammals [9, 16–18]. However, the specific mechanisms by which *Bacillus* spp. enhance resistance to viral infection in early vertebrates like teleost fish remain poorly understood.

Hence, we further isolated a Bv strain from the intestinal mucosa of largemouth bass and characterized its digestive and antibacterial properties. Hematological parameters and biochemical indices serve as valuable biological indicators to assess the health status and physiological condition of fish [42]. In our study, we found that supplementation with Bv significantly increased the activity of digestive and immune enzymes and decreased mortality from viral infections. This suggests that Bv supplementation activated and promoted the metabolic and immune functions of the bass. Previous studies in humans have reported that probiotics provide multiple beneficial effects by modulating mucosal immunity, microbiota composition, and metabolism [43, 44]. Transcriptome sequencing further revealed that the highest number of differentially expressed genes was observed in HG, and the expression profiles of immune and metabolic-related genes across different intestinal segments exhibited heterogeneity. Immune and metabolism-related genes in FG and HG showed uniqueness, suggesting functional differences in immune and metabolic processes. KEGG analysis indicated a higher enrichment of immune-related pathways in HG and MG, with particularly enrichment in HG. This is consistent with previous findings in fish, where nutrient uptake progressively decreases, and the importance of immune homeostasis mechanisms increases from the FG to the HG [45–47].

A previous study demonstrated that *Bacillus* spp. affect the gene expression of the gastrointestinal immune system in fish primarily through symbiotic host-microbiome interactions [48, 49]. We further assessed the composition and structure characteristics of the gut microbiota

using 16S rRNA analysis. The Chao1 index indicated that Bv supplementation induced a significant increase in microbial richness in the HG, as reported in a previous study in *Cyprinus carpio* Songpu mirror [50]. Moreover, we found that Firmicutes were significantly increased in HG, which could contribute to an increase in the Firmicutes/Bacteroidetes ratio. Notably, a reduction in the Firmicutes/Bacteroidetes ratio is known to be associated with dysbiosis and inflammatory diseases [51, 52]. Proteobacteria are known to encompass a wide variety of pathogens with invasive properties, which were observed to significantly decrease in both the FG and MG [53, 54]. Previous studies reported that probiotic administration enhances microbial balance in humans by regulating the abundance of beneficial and harmful bacteria [55]. Our findings show that Bv supplementation resulted in a decrease in *Aeromonas* abundances, which have been associated with disease in farmed fish [56]. Moreover, we observed a significant increase in beneficial bacteria such as *Cetobacterium* and *Bacillus*, which have been demonstrated to play a crucial role in regulating host health and maintaining mucosal homeostasis in aquaculture [57–59].

In mammals, microbiotas modulate mucosal immunity through the production of secondary metabolites, thereby influencing the host's susceptibility to infection [60]. In our study, the differential metabolites induced by Bv supplementation enriched pathways related to immune and metabolic functions, particularly in HG. This is consistent with the variation observed in the transcriptome analysis, suggesting that Bv supplementation induced a robust immune response in HG. Correlation analysis further showed a positive correlation between *Bacillus* spp. and DG metabolite in the HG. Genomic analysis indicated that *Bacillus* spp. can regulate the production of DG through triacylglycerol lipase (TAG lipase) [61]. Importantly, we found that the immune-related pathways were significantly enriched in both transcriptomic and metabolomic association analyses, with DG being one of the most crucial metabolites. The NF- κ B pathway plays an important regulatory role in the immune response to infection, and studies in mammals reported that probiotics stimulate the NF- κ B signaling pathway, activating downstream signaling factors that regulate innate and adaptive immune functions [62–64]. Critically, we found that DG exerts a protective role in enhancing the antiviral response of EPC cells and reducing the mortality rate of largemouth bass through elevating the expression of antiviral genes, which is consistent with studies in mammals that DG mediates the NF- κ B signaling pathway to combat viral invasion by upregulating the expression of *ifna*, *isg15*, and *mx* [65, 66]. To our knowledge, our study provides the first evidence that

Bacillus spp. are a core microbiota in resisting viral infections and reveals its potential mechanism of antiviral infection in teleost fish.

Conclusion

In this study, we identified *Bacillus* spp. as a core contributor that mediates the clinical symptoms of early antiviral infection in largemouth bass. The feeding trials further confirmed that feeding Bv provides various benefits to the host, including promoting growth performance, enhancing immune enzyme activity, and reducing mortality in largemouth bass following LMBV infection. Multi-omics analysis suggested that *Bacillus* spp. confer protection through an enhanced mucosal immune response, improved composition of intestinal commensal microbiota, and altered host metabolism, particularly within the HG. Notably, Bv facilitates enzymatic hydrolysis to produce DG, an endogenous intermediate of lipid metabolism that enhances the resistance of cells to viral infection through the activation of antiviral genes. Consistently, DG supplementation decreased the mortality and clinical phenotypes of infected largemouth bass. These results provide evidence that *Bacillus* spp. are a core microbiota that mediates early antiviral infection in largemouth bass, which confers resistance to viral infections by regulating the production of DG during lipid metabolism. Overall, our findings suggest that *Bacillus* spp. emerge as core microbiota against viral infections in early vertebrates, supporting the evolutionary viewpoint that probiotics play conserved roles as core microbiota in regulating microbial homeostasis and mucosal immunity across the vertebrate lineage.

Materials and methods

Fish

All largemouth bass used in the experiments were obtained from a fish farm in Wuhan (China). They were soaked for 30 min in a tank containing 10 mg/L of potassium permanganate and then maintained in a recirculating aquaculture system for more than 4 weeks at a temperature of 28 °C. The fish were fed daily with commercial diets. Prior to the formal experiment, we randomly selected largemouth bass for PCR testing to confirm the absence of LMBV infection and comprehensively assessed their health status by evaluating external symptoms.

Infection of fish with largemouth bass virus (LMBV) and phenotype definition

Healthy largemouth bass were randomly divided into two groups: a control (Ctrl) group and an infected group ($n = 150$). Fish in the infected group were exposed to an infective dose of 5 ml of LMBV (1×10^7 TCID₅₀) diluted in 5

L of water at 28 °C for 4 h. The Ctrl group was exposed to virus-free cell culture supernatant under the same treatment conditions. Following exposure, both groups of fish were transferred to new freshwater tanks for culture. Before sampling, largemouth bass were anesthetized using MS-222, and tissues were collected at 1, 4, 7, 14, 21, and 28 days post-infection (DPI) for further experiments. Gut samples were collected and pooled at 7 DPI, with each sample containing gut tissue from three fish for 16S sequencing.

Phenotype definition

The infected fish showed detectable LMBV load and exhibited classic clinical phenotype (splenomegaly, skin ulcers, and fin congestion). We then defined one star to represent the appearance of a clinical phenotype once, two stars to represent the appearance of the clinical phenotype twice, and three stars to indicate the presence of all three clinical phenotypes in the infected fish simultaneously. In phenotype assessment, the mild phenotype is represented by zero or one star, while the severe phenotype is represented by two or three stars.

B. velezensis (Bv) feeding experiment

To investigate the effects of Bv on the resistance of largemouth bass to viral infection, fish were randomly divided into two groups: the Ctrl group and the Bv-supplemented group ($n = 150$). Briefly, Bv was cultured in LB liquid medium for 3 days and then sprayed onto commercial feeds, allowed to dry naturally, and stored at 4 °C. Bass were fed either a Ctrl diet or a Bv-supplemented diet ($1-3 \times 10^8$ CFU/g diet) at 4% of their body weight, with the feeding strategy adjusted every 2 weeks according to their feed intake. After 28 days of feeding, growth parameters, including specific growth rate (SGR), feed conversion rate (FCR), and weight gain rate (WGR), were calculated for both groups according to methods described in a previous study [67]. Tissue samples from fish in each group were randomly collected ($n = 20$) and stored at -80 °C for enzyme activity analysis, as well as for 16S, transcriptomic, and metabolomic sequencing. Each sample used for sequencing consisted of gut tissue from three fish. A total of 30 fish were intraperitoneally injected with a cell suspension containing LMBV for the mortality test, and cumulative mortality was recorded daily for 30 days. The mortality experiment was repeated twice. Meanwhile, the remaining fish ($n = 60$) were injected with 100- μ L LMBV suspension (1×10^7 TCID₅₀, 1:1000) and sacrificed at 7 DPI for sample collection and statistical analysis of pathological phenotypes. **Phenotype definition.**

The infected fish showed detectable LMBV load and exhibited clinical phenotype (severe abdominal redness and swelling, skin ulcers). Fish were classified based on

the severity of symptoms using a star rating system. In phenotype assessment, the non-phenotype is represented by zero star, the mild phenotype is represented by one star, while the severe phenotype is represented by two stars.

Diglyceride (DG) feeding experiment

The bass were randomly divided into two groups: the Ctrl group and the DG-supplemented group ($n = 150$ fish). Bass were fed either a Ctrl diet or a DG-supplemented diet (0.5% concentration) at 4% of their body weight, with feeding strategies adjusted every 2 weeks. After feeding a regimen of 4 weeks, a total of 30 fish per group were intraperitoneally injected with a cell suspension containing LMBV (1×10^7 TCID₅₀, 1:1000) for the mortality test, and cumulative mortality was recorded daily for 30 days. The mortality experiment was repeated twice. Meanwhile, the fish ($n = 60$) were all injected with LMBV and sacrificed at 7 DPI for sample collection and statistical analysis of pathological phenotypes. DG powder (> 70%) was obtained from Xi'an Shouhe Biotechnology Co., Ltd.).

Virus neutralization experiment of DG in vitro

We performed viral neutralization experiments in vitro to evaluate the ability of DG to enhance the resistance of EPC to LMBV infections. Briefly, EPC cells were seeded into 12-well plates and cultured overnight. The cells were then incubated with 500 μ L of M199 solution containing 0.5% DG for 2 h. The Ctrl group was incubated with M199. After being washed three times with PBS, the LMBV suspension (1×10^7 TCID₅₀) was diluted (500 μ L, 1:1000) and incubated with the EPC cells for 2 h at 28 °C. Subsequently, the infected cells were washed three times with PBS and cultured in 1% FBS/M199 at 28 °C for 24 h. Finally, the infected EPC cells were used for the detection of LMBV load and analysis of the cytopathic effect (CPE).

RNA isolation, DNA extraction, and qPCR analysis

The method of total RNA extraction and qPCR protocol was carried out according to previous studies [36]. In brief, total RNA was isolated from the gut of largemouth bass using the TRIzol reagent (Tsingke, Beijing, China). A total of 1- μ g RNA was used to synthesize cDNA; subsequently, the cDNA was diluted threefold for qPCR analysis. To quantify the LMBV load in tissues, the genomic DNA was extracted using the DNA extract kit (CW BIO, Beijing, China) according to the manufacturer's instructions. A standard curve was constructed using an LMBV plasmid, and LMBV loads were calculated by extrapolating the average values to the curve. The qPCR primers used in this study are provided in Table S1.

Light microscopy and immunofluorescence microscopy studies

Gut tissues from infected largemouth bass at different time points were fixed in 4% neutral buffered formalin for at least 1 day. The tissues were gradually dehydrated and embedded in paraffin and cut into 5- μ m slices. For histomorphologic examination, the gut sections were stained with H&E solution according to the methods previously described [68]. Fluorescence in situ hybridization analysis was performed according to the method described in a previous study [69].

Flow cytometry analysis

In our study, flow cytometry was used to evaluate the proportion and quantity of intestinal bacteria. Briefly, intestinal mucosal tissue samples were scraped using sterile phosphate-buffered saline (PBS) to collect microbes, followed by filtration through a 100- μ m cell strainer. The supernatant was collected and centrifuged three times for 5 min at 400 g, followed by centrifugation to collect the precipitate at 13,000 g. Finally, the microbiota was collected and incubated in 200 μ L of PBS containing SYTO BC, and an equal volume bacterial solution was used for bacterial enumeration using a CytoFLEX LX Flow Cytometer.

Determination of antimicrobial and enzyme-producing capacity of Bv

The antimicrobial activity of Bv was assessed using a modified agar spot method as previously described [70]. Three bacteria including *A. hydrophila*, *E. piscicida*, and *N. seriolae* were selected as pathogenic strains to assess the antimicrobial ability of Bv [71]. In the Bv feeding experiment, feeding was terminated 3 days before the sacrifice procedure. Subsequently, the gut and blood samples from the Ctrl and Bv groups were collected for enzyme activity detection ($n = 9$). Serum supernatant was collected after centrifugation at 6000 \times g for 8 min and stored at -80 °C. The activities of superoxide dismutase (SOD), lysozyme (LSZ), acid phosphatase (ACP), trypsin (TPS), amylase (AMS), and lipase (LPS) were assessed using standard biochemical assays. The activities of SOD, LSZ, and LPS were assessed using colorimetric assays, while ACP, TPS, and AMS were measured using substrate hydrolysis assays following the manufacturer's instructions (Nanjing Jiancheng, Nanjing, China).

RNA-seq library preparation, sequencing, and data analysis

RNA-seq libraries of the FG, MG, and HG tissues from the Ctrl and Bv fed groups were constructed and analyzed by Majorbio Bio-Pharm Technology Co. Ltd. (Shanghai, China). The libraries were sequenced on the

Illumina HiSeq X Ten or NovaSeq 6000 platform, producing paired-end reads of 150 bp in length. Raw reads were trimmed and mapped to the largemouth bass genome using Spliced Transcripts Alignment to a Reference (STAR) with default parameters. Genes were considered differentially expressed (DEGs) if they met the criteria of a false discovery rate (FDR) ≤ 0.05 and $|\log_2(\text{fold-change})| \geq 1$.

Extraction, annotation, and analysis of gut metabolites

The gut samples of the Ctrl and Bv groups were sent to Majorbio Bio-Pharm Technology Co. Ltd. (Shanghai, China). The metabolites from gut contents were extracted, detected, and annotated following the method previously described [72]. Metabolite annotation was carried out using the Automatic Mass Spectral Deconvolution and Identification System, with database searches conducted against resources such as the National Institute of Standards and Technology and the Wiley Registry Metabolomics Database. The data were then adjusted based on the internal standard for subsequent analysis.

Bacterial 16S rRNA sequencing and data analysis

The gut samples of the Ctrl and the Bv group were sent to Majorbio Bio-Pharm Technology Co. Ltd. (Shanghai, China) for 16S sequence analysis. The methods used in this study are as described in previous studies [36].

Statistics

The differences between the groups were analyzed using Prism version 6.0 (GraphPad Software). Unpaired Student's *t*-test (Prism version 8.0; GraphPad) and one-way analysis of variance with Bonferroni correction were used for the analysis of differences between groups. Data are expressed as mean \pm standard error of the mean (SEM), with *p*-values < 0.05 regarded as statistically significant.

Supplementary Information

The online version contains supplementary material available at <https://doi.org/10.1186/s40168-025-02124-8>.

Supplementary Material 1. Figure 1. A Phenotypic definition of largemouth bass after viral infection. (Left: Mild group, right: Severe group. The symptoms observed in infected fish included enlarged spleen, skin ulceration and fin hyperemia. Red and black arrows highlight areas associated with the symptoms. One star represents the appearance of a phenotype once, two stars represent the appearance of the phenotype twice, and three stars indicate the presence of all three phenotypes in the infected fish simultaneously. The mild phenotype was indicated by one star, and the severe phenotype by two or three stars in the phenotypic scoring system. B qPCR was used to quantify LMBV mcp gene copies (\log_{10}) in the HK of fish in the Ctrl, Mild, and Severe groups ($n = 6$). C Expression levels of immune-related genes in fish at 1, 4, Mild-7, Severe-7, 14, 21, and 28 DPI. D Flow cytometry analysis of microbiota stained without SYTO BC Green. Statistical differences were evaluated by unpaired Student's *t* test. Data are presented as mean \pm SEM of three biological duplicated.

P* < 0.05, *P* < 0.01, and ****P* < 0.001. Figure 2. A Bacteriostatic ability of the screened *Bacillus velezensis* (Bv) against *Aeromonas hydrophila* (*A. hydrophila*), *Edwardsiella piscicida* (*E. piscicida*), and *Nocardia seriolae* (*N. seriolae*). B Statistical chart showing the fold change in the inhibition of three pathogenic bacteria. C Production of digestive enzymes (amylase, cellulase, protease, and lipase) by Bv. Figure 3. A Histological examination of FG, MG and HG in Ctrl and Bv-supplemented group fish at 28 days was analyzed via H&E staining. Scale bars, 50 μm . B Statistical analysis of villi number, villi length, and muscle layer thickness in the FG, MG and HG in the Ctrl and Bv-supplemented groups ($n = 6$). Data are representative of at least three independent experiments (mean \pm SEM). C Activities of LSZ, SOD, and ACP in the FG, MG, and HG of the Ctrl and Bv-supplemented groups ($n = 8$). D Definition of non, mild, and severe symptoms in largemouth bass infected with LMBV by injection. Indicators include severe abdominal redness and swelling, skin ulcers. Black arrows highlight areas corresponding to the symptoms. In phenotype assessment, the non-phenotype is represented by zero star, the mild phenotype is represented by one star, while the severe phenotype is represented by two stars. Statistical differences were evaluated by unpaired Student's *t* test. Data are presented as mean \pm SEM of three biological duplicated. **P* < 0.05, ***P* < 0.01, and ****P* < 0.001. Figure 4. Venn diagram and OTU numbers of microbiota in FG, MG, and HG of fish in the Ctrl and Bv-supplemented groups. Figure 5. Genome analysis reveals the ability of Bv to synthesize lipases. Figure 6. A ImageJ was used to quantify the CPE area in the Ctrl and 0.5% DG group ($n = 6$). B Experimental strategy for dietary supplementation with DG. Largemouth bass were fed with commercial feed containing PBS or DG (0.5%), injected with LMBV at 28 DPI and sacrificed at 7 DPI for tissue sample collection. Statistical differences were evaluated by unpaired Student's *t* test. (**p* < 0.05, ***p* < 0.01, ****p* < 0.001). Supplementary tables: Table S1. Primers used in this study. Table S2. Metabolite enrichment pathway in the HG.

Acknowledgements

We express our gratitude to Yan Wang and Yuan Sun from the Institute of Hydrobiology, Chinese Academy of Sciences, for their valuable assistance with the flow cytometry analysis procedures.

Authors' contributions

G.C. designed the overall experiment and wrote the original manuscript; W.K, R.L, X.Q. and Z.J. conducted most of the experiments; Y.S, P.Y, X.C and L.X performed experiments and corrected format; Z.X. supervised the execution of this study.

Funding

This work was supported by grants from the National Natural Science Foundation of China (32225050, U24 A20461, 32303053), the Strategic Priority Research Program of the Chinese Academy of Sciences (XDB0730100), the Hubei Provincial Natural Science Foundation of China (2023 AFA002), and the Natural Science Foundation of Wuhan (2024040701010071).

Data availability

No datasets were generated or analysed during the current study.

Ethics approval and consent to participate

All fish-related procedures were conducted following the Guiding Principles for the Care and Use of Laboratory Animals and were approved by the Institute of Hydrobiology, Chinese Academy of Sciences (permit number 2019–048).

Consent for publication

Not applicable.

Competing interests

The authors declare no competing interests.

Author details

¹Department of Aquatic Animal Medicine, College of Fisheries, Huazhong Agricultural University, Wuhan, Hubei 430070, China. ²State Key Laboratory of Breeding Biotechnology and Sustainable Aquaculture, Institute

of Hydrobiology, Chinese Academy of Sciences, Wuhan 430072, China. ³Liaoning Key Laboratory of Marine Animal Immunology, Dalian Ocean University, Dalian 116023, China.

Received: 11 January 2025 Accepted: 27 April 2025

Published online: 16 May 2025

References

- Colston TJ, Jackson CR. Microbiome evolution along divergent branches of the vertebrate tree of life: what is known and unknown. *Mol Ecol*. 2016;25:3776–800.
- Afzaal M, Saeed F, Shah Y, Hussain M, Rabail R, Socol C, et al. Human gut microbiota in health and disease: unveiling the relationship. *Front Microbiol*. 2022;13: 999001.
- Lo B, Chen G, Núñez G, Caruso R. Gut microbiota and systemic immunity in health and disease. *Int Immunol*. 2021;33:197–209.
- Hou K, Wu Z, Chen X, Wang J, Zhang D, Xiao C, et al. Microbiota in health and diseases. *Signal Transduct Target Ther*. 2022;7:135.
- Wu H, Wu E. The role of gut microbiota in immune homeostasis and autoimmunity. *Gut Microbes*. 2012;3:4–14.
- Sharon I, Quijada NM, Pasolli E, Fabbri M, Vitali F, Agamennone V, et al. The core human microbiome: does it exist and how can we find it? A critical review of the concept. *Nutrients*. 2022;14:2872.
- Wu G, Xu T, Zhao N, Lam YY, Ding X, Wei D, et al. A core microbiome signature as an indicator of health. *Cell*. 2024;187:6550–65.
- Zhang J, Guo Z, Xue Z, Sun Z, Zhang M, Wang L, et al. A phylo-functional core of gut microbiota in healthy young Chinese cohorts across lifestyles, geography and ethnicities. *ISME J*. 2015;9:1979–90.
- Yan Z, Hao T, Yan Y, Zhao Y, Wu Y, Tan Y, et al. Quantitative and dynamic profiling of human gut core microbiota by real-time PCR. *Appl Microbiol Biotechnol*. 2024;108:396.
- Grond K, Sandercock BK, Jumpponen A, Zeglin LH. The avian gut microbiota: community, physiology and function in wild birds. *J Avian Biol*. 2018;49: e01788.
- Siddiqui R, Maciver SK, Khan NA. Gut microbiome-immune system interaction in reptiles. *J Appl Microbiol*. 2022;132:2558–71.
- Luan Y, Li M, Zhou W, Yao Y, Yang Y, Zhang Z, et al. The fish microbiota: research progress and potential applications. *Engineering*. 2023;29:137–46.
- Kokou F, Sasson G, Friedman J, Eyal S, Ovadia O, Harpaz S, et al. Core gut microbial communities are maintained by beneficial interactions and strain variability in fish. *Nat Microbiol*. 2019;4:2456–2465.
- Petrariu O, Barbu I, Niculescu A, Constantin M, Grigore G, Cristian R, et al. Role of probiotics in managing various human diseases, from oral pathology to cancer and gastrointestinal diseases. *Front Microbiol*. 2024;14:1296447.
- Shi S, Liu J, Dong J, Hu J, Liu Y, Feng J, et al. Research progress on the regulation mechanism of probiotics on the microecological flora of infected intestines in livestock and poultry. *Lett Appl Microbiol*. 2022;74:647–55.
- Edouard S, Million M, Bachar D, Dubourg G, Michelle C, Ninove L, et al. The nasopharyngeal microbiota in patients with viral respiratory tract infections is enriched in bacterial pathogens. *Eur J Clin Microbiol Infect Dis*. 2018;37:1725–33.
- Bae M, Cassilly CD, Liu X, Park SM, Tusi BK, Chen X, et al. *Akkermansia muciniphila* phospholipid induces homeostatic immune responses. *Nature*. 2022;608:168–73.
- Yoshida N, Emoto T, Yamashita T, Watanabe H, Hayashi T, Tabata T, et al. *Bacteroides vulgatus* and *Bacteroides dorei* reduce gut microbial lipopolysaccharide production and inhibit atherosclerosis. *Circulation*. 2018;138:2486–98.
- Zhuang Y, Gao D, Jiang W, Xu Y, Liu G, Hou G, et al. Core microbe *Bifidobacterium* in the hindgut of calves improves the growth phenotype of young hosts by regulating microbial functions and host metabolism. *Microbiome*. 2025;13(1):13.
- Wang B, Yao M, Lv L, Ling Z, Li L. The human microbiota in health and disease. *Engineering*. 2017;3:71–82.
- Maffei N, Raileanu C, Balta A, Ambrose L, Boev M, Marin D, et al. The potential impact of probiotics on human health: an update on their health-promoting properties. *Microorganisms*. 2024;12:234.
- Qi X, Zhang Y, Zhang Y, Luo F, Song K, Wang G, et al. Vitamin B₁₂ produced by *Cetobacterium somerae* improves host resistance against pathogen infection through strengthening the interactions within gut microbiota. *Microbiome*. 2023;11:135.
- Wang X, Hu W, Zhu L, Yang Q. *Bacillus subtilis* and surfactin inhibit the transmissible gastroenteritis virus from entering the intestinal epithelial cells. *Biosci Rep*. 2017;37: BSR20170082.
- Wang X, Hao G, Zhou M, Chen M, Ling H, Shang Y. Secondary metabolites of *Bacillus subtilis* L2 show antiviral activity against pseudorabies virus. *Front Microbiol*. 2023;14:1277782.
- Scopel e Silva D, de Castro CC, da Silva e Silva F, Sant'anna V, Vargas GD, de Lima M, et al. Antiviral activity of a *Bacillus* spp. P34 peptide against pathogenic viruses of domestic animals. *Braz J Microbiol*. 2014;45:1089–1094.
- Song K, Luo F, Chen W, Qi X, Shen Y, Zha J, et al. Evaluation on the antiviral activity of *Bacillus velezensis* extract against spring viremia of carp virus. *Aquaculture*. 2022;547: 737477.
- Ringø E, Harikrishnan R, Soltani M, Ghosh K. The effect of gut microbiota and probiotics on metabolism in fish and shrimp. *Animals (Basel)*. 2022;12:3016.
- Ganesan S, Ponce M, Shabits B, Tavassoli M, Zaremborg V. Diacylglycerol links lipid droplets and tubular ER during growth resumption from stationary phase. *FASEB J*. 2019;33:488–96.
- Zhong X, Guo R, Zhou H, Liu C, Wan C. Diacylglycerol kinases in immune cell function and self-tolerance. *Immunol Rev*. 2008;224:249–64.
- Zhang Y, Gui B, Jia ZH, Li YM, Liao LJ, Zhu ZY, et al. Artificial infection pathway of largemouth bass LMBV and identification of resistant and susceptible individuals. *Aquaculture*. 2024;582: 740527.
- Ortega-Villaizán M, Mercado L, Chico V. Editorial: Antiviral immune response in fish and shellfish. *Front Immunol*. 2023;14:1155538.
- Magnadottir B. Immunological control of fish diseases. *Mar Biotechnol*. 2010;12:361–79.
- Liu Y, Yan LM, Wan L, Xiang TX, Le A, Liu JM, et al. Viral dynamics in mild and severe cases of COVID-19. *Lancet Infect Dis*. 2020;20:656–7.
- Hu S, Bourgonje AR, Gacesa R, Jansen BH, Björk JR, Bangma A, et al. Mucosal host-microbe interactions associate with clinical phenotypes in inflammatory bowel disease. *Nat Commun*. 2024;15:1470.
- Huang C, Wang Y, Li X, Ren L, Zhao J, Hu Y, et al. Clinical features of patients infected with 2019 novel coronavirus in Wuhan. *China Lancet*. 2020;395:497–506.
- Kong W, Cheng G, Cao J, Yu J, Wang X, Xu Z. Ocular mucosal homeostasis of teleost fish provides insight into the coevolution between microbiome and mucosal immunity. *Microbiome*. 2024;12:23.
- Qiu P, Ishimoto T, Fu L, Zhang J, Zhang Z, Liu Y. The gut microbiota in inflammatory bowel disease. *Front Cell Infect Microbiol*. 2022;12: 733992.
- DeGruttola AK, Low D, Mizoguchi A, Mizoguchi E. Current understanding of dysbiosis in disease in human and animal models. *Inflamm Bowel Dis*. 2016;22:1137–50.
- André AC, Debande L, Marteyn BS. The selective advantage of facultative anaerobes relies on their unique ability to cope with changing oxygen levels during infection. *Cell Microbiol*. 2021;23: e13338.
- Alanazi A, Younas S, Ejaz H, Zainab Mazhari BB, Abosalif K, Abdalla AE, et al. Exploration of the human microbiome's role in health and disease through the lens of genetics. *J Pure Appl Microbiol*. 2024;18(3):1413–23.
- Ha S, Wong VW, Zhang X, Yu J. Interplay between gut microbiome, host genetic and epigenetic modifications in MASLD and MASLD-related hepatocellular carcinoma. *Gut*. 2024;74(1):141–52.
- Adams, S. Marshall, AM. Brown, RW. A quantitative health assessment index for rapid evaluation of fish condition in the field. *T Am Fish Soc*. 1993;122:63–73.
- Mazziotta C, Tognon M, Martini F, Torreggiani E, Rotondo JC. Probiotics mechanism of action on immune cells and beneficial effects on human health. *Cells*. 2023;12(1):184.
- Liu Y, Wang J, Wu C. Modulation of gut microbiota and immune system by probiotics, pre-biotics, and post-biotics. *Front Nutr*. 2022;8: 634897.
- Løkka G, Austbø L, Falk K, Bromage E, Fjellidal PG, Hansen T, et al. Immune parameters in the intestine of wild and reared unvaccinated and vaccinated Atlantic salmon (*Salmo salar* L.). *Dev Comp Immunol*. 2014;47(1):6–16.

46. López Nadal A, Ikeda-Ohtsubo W, Sipkema D, Peggs D, McGurk C, Forlenza M, et al. Feed, microbiota, and gut immunity: using the zebrafish model to understand fish health. *Front Immunol.* 2020;11:114.
47. Wang Z, Du J, Lam SH, Mathavan S, Matsudaira P, Gong Z, et al. Morphological and molecular evidence for functional organization along the rostrocaudal axis of the adult zebrafish intestine. *BMC Genomics.* 2010;11:392.
48. Shija VM, Amoah K, Cai J. Effect of bacillus probiotics on the immunological responses of Nile tilapia (*Oreochromis niloticus*): a review. *Fishes.* 2023;8:366.
49. Lee PT, Yamamoto FY, Low CF, Loh JY, Chong CM. Gut immune system and the implications of oral-administered immunoprophylaxis in finfish aquaculture. *Front Immunol.* 2021;12: 773193.
50. Luo L, Xu Q, Xu W, Li J, Wang C, Wang L, et al. Effect of *Bacillus megaterium*-coated diets on the growth, digestive enzyme activity, and intestinal microbial diversity of Songpu mirror carp (*Cyprinus specularis Songpu*). *Biomed Res Int.* 2020;2020:8863737.
51. Ma Y, Wang W, Zhang H, Wang J, Zhang W, Gao J, et al. Supplemental *Bacillus subtilis* DSM 32315 manipulates intestinal structure and microbial composition in broiler chickens. *Sci Rep.* 2018;8:15358.
52. Stojanov S, Berlec A, Štrukelj B. The influence of probiotics on the Firmicutes/Bacteroidetes ratio in the treatment of obesity and inflammatory bowel disease. *Microorganisms.* 2020;8:1715.
53. Rizzatti G, Lopetuso LR, Gibiino G, Binda C, Gasbarrini A. Proteobacteria: a common factor in human diseases. *Biomed Res Int.* 2017;2017:9351507.
54. Shi Y, Kong W, Gong F, Cai C, Zhang Y, Cheng G, et al. Yeast β -glucan enhances the intestinal immune function in coho salmon via the modulation of gut microbiota-mediated lipid metabolism. *Aquaculture.* 2025;599: 742123.
55. Wierzbicka A, Mańkowska-Wierzbicka D, Mardas M, Stelmach-Mardas M. Role of probiotics in modulating human gut microbiota populations and activities in patients with colorectal cancer—a systematic review of clinical trials. *Nutrients.* 2021;13:1160.
56. Chen F, Sun J, Han Z, Yang X, An JA, Lv A, Hu X, Shi H, et al. Isolation, identification and characteristics of *Aeromonas veronii* from diseased crucian carp (*Carassius auratus gibelio*). *Front Microbiol.* 2019;10:2742.
57. Kuebutornye FKA, Abarike ED, Lu Y. A review on the application of *Bacillus* as probiotics in aquaculture. *Fish Shellfish Immunol.* 2019;87:820–8.
58. Colorado Gómez MA, Melo-Bolívar JF, Ruiz Pardo RY, Rodríguez JA, Villamil LM. Unveiling the probiotic potential of the anaerobic bacterium *Cetobacterium* spp. nov. C33 for enhancing Nile tilapia (*Oreochromis niloticus*) cultures. *Microorganisms.* 2023;11:2922.
59. Vijayaram S, Chou C, Razafindralambo H, Ghafarifarsani H, Divsalar E, Van Doan H, et al. *Bacillus* spp. as potential probiotics for use in tilapia fish farming aquaculture—a review. *Ann Animal Sci.* 2024;24(4):995–1006.
60. Campbell C, Kandalgaonkar MR, Golonka RM, Yeoh BS, Vijay-Kumar M, Saha P, et al. Crosstalk between gut microbiota and host immunity: impact on inflammation and immunotherapy. *Biomedicines.* 2023;11:294.
61. Li X, Benning C, Kuo MH. Rapid triacylglycerol turnover in *Chlamydomonas reinhardtii* requires a lipase with broad substrate specificity. *Eukaryot Cell.* 2012;11:1451–62.
62. Liu T, Zhang L, Joo D, Sun SC. NF- κ B signaling in inflammation. *Signal Transduction Targeted Ther.* 2017;2:1–9.
63. Balachandran S, Beg AA. Defining emerging roles for NF- κ B in antiviral responses: revisiting the interferon- β enhanceosome paradigm. *PLoS Pathog.* 2011;7: e1002165.
64. Kim DH, Jeong M, Kim JH, Son JE, Lee JY, Park SJ, et al. *Lactobacillus salivarius* HHuMin-U activates innate immune defense against norovirus infection through TBK1-IRF3 and NF- κ B signaling pathways. *Research.* 2022;2022:0007.
65. Shin J, O'Brien TF, Grayson JM, Zhong XP. Differential regulation of primary and memory CD8 T cell immune responses by diacylglycerol kinases. *J Immunol.* 2012;188:2111–7.
66. Raftery N, Stevenson NJ. Advances in anti-viral immune defense: revealing the importance of the IFN JAK/STAT pathway. *Cell Mol Life Sci.* 2017;74:2525–35.
67. Zhang S, Wang C, Liu S, Wang Y, Lu S, Han S, et al. Effect of dietary phenylalanine on growth performance and intestinal health of triploid rainbow trout (*Oncorhynchus mykiss*) in low fishmeal diets. *Front Nutr.* 2023;10:1008822.
68. Yu Y, Huang Z, Kong W, Dong F, Zhang X, Zhai X, et al. Teleost swim bladder, an ancient air-filled organ that elicits mucosal immune responses. *Cell Discov.* 2022;8:31.
69. Xu Z, Takizawa F, Casadei E, Shibasaki Y, Ding Y, Sauters TJ, et al. Specialization of mucosal immunoglobulins in pathogen control and microbiota homeostasis occurred early in vertebrate evolution. *Sci Immunol.* 2020;5:3254.
70. Fleming HP, Etchells JL, Costilow RN. Microbial inhibition by an isolate of pediococcus from cucumber brines. *Appl Microbiol.* 1975;30:1040–2.
71. Xia L, Cheng G, Wang P, Dong Z, Mu Q, et al. Screening and identification of probiotics from the intestinal tract of largemouth bass (*Micropterus salmoides*) for use as a feed additive and bacterial infection control. *Aquaculture.* 2024;584: 740661.
72. Wu Z, Zhang Q, Lin Y, Hao J, Wang S, Zhang J, et al. Taxonomic and functional characteristics of the gill and gastrointestinal microbiota and its correlation with intestinal metabolites in NEW GIFT strain of farmed adult Nile tilapia (*Oreochromis niloticus*). *Microorganisms.* 2021;9:617.

Publisher's Note

Springer Nature remains neutral with regard to jurisdictional claims in published maps and institutional affiliations.